CORROSION SCIENCE AND TECHNOLOGY, Vol.24, No.6(2025), pp.539~557 pISSN 1598-6462 / eISSN 2288-6524
[Review Paper] DOI: https://doi.org/10.14773/cst.2025.24.6.539

Elucidation of Corrosion Mechanism in a Simulated Potable Water of 304 stainless steel for Water Storage Tank

Jae-Hyeok Choi[1], Seung-Heon Choi[1], Sang-Shin Lee[1], Young-Ran Yoo[2], Hyun-Hak Cho[3], Young-Cheon Kim[1,4,†], and Young-Sik Kim[4]

[1]*Department of Material Science and Engineering, Gyeongkuk National University, 1375 Gyeongdong-ro, Andong, Gyeongbuk 36729, Republic of Korea*
[2]*Department of Semiconductor Equipment, Gumi campus of Korea Polytechnic, 84 Suchul-daero 3-gil, Gumi, Gyeongbuk, 39377, Republic of Korea*
[3]*Department of Intelligent Energy Engineering, Gwangju campus of Korea Polytechnic, 85 Haseo-ro, Gwangju, 61099, Republic of Korea*
[4]*Materials Research Center for Energy and Clean Technology, Gyeongkuk National University, 1375 Gyeongdong-ro, Andong, Gyeongbuk, 36729, Republic of Korea*
(Received December 10, 2025; Revised December 19, 2025; Accepted December 19, 2025)

Drinking water storage tanks are essential for maintaining water quality in distribution systems, and their stability is crucial. STS 304 stainless steel, known for its excellent corrosion resistance, is commonly used in water supply facilities and storage tanks. However, localized corrosion has been observed in STS 304 tanks, likely due to local enrichment of chloride (Cl^-) or residual chlorine (OCl^-) ions caused by evaporation and condensation. This study evaluated the corrosion behavior of STS 304 base metal and weld metal in simulated potable water containing 50 ppm, 200 ppm, or 400 ppm Cl^- and 2 ppm, 4 ppm, or 8 ppm OCl^- at temperatures of 20 °C, 35 °C, and 50 °C. To assess corrosion resistance, we conducted cyclic polarization, open-circuit potential (OCP) measurements, and electrochemical impedance spectroscopy (EIS). While increases in $Cl^-$and OCl^- ions had minimal impact on pitting and protection potentials, higher temperatures led to a decrease in pitting potential. The addition of OCl^- caused a rapid increase in OCP to a level between the protection and pitting potentials, indicating that the corrosion observed in 304 tanks is linked to the potential-raising effect of OCl^- ion addition.

Keywords: *Potable water tanks, 304 Stainless steel, Hypochlorite (OCl^-), Pitting potential, Protection potential*

1. Introduction

Since river water contains various microorganisms and suspended solids, it must undergo appropriate water treatment processes before it is used for drinking. In water treatment processes, raw water is subjected to mixing, coagulation, sedimentation, and filtration, followed by disinfection to inactivate pathogens [1-3]. Drinking water supply systems include various storage facilities and conveyance equipment to supply the treated water reliably to facilities and households, and among these, water tanks store the treated water from water treatment plants and play an important role in maintaining water quality and providing a stable water supply [4,5]. Various materials such as plastic and concrete have been used for water tanks; however, in recent years the use of stainless steel has increased because it is advantageous in terms of hygienic management and durability [6-8].

In general, in seawater or brine environments, localized corrosion of stainless steels increases as the temperature and Cl^- concentration in the solution increase [9-11]. This is because the aggressive Cl^- ions penetrate defects in the passive film and accelerate local film breakdown, while the dissolution of exposed metal ions causes a decrease in pH inside the pit and, together with the continuous ingress and accumulation of Cl^-, promotes pit propagation [12,13]. However, under domestic drinking water conditions, chloride (Cl^-) is controlled at levels up to

†Corresponding author: kimyc@gknu.ac.kr
J. H. Choi: Master's degree student, S. S. Lee: Master's degree student, S. H. Choi: Ph.D. candidate, Y. R. Yoo: Professor, H. H. Cho: Professor, Y. C. Kim: Professor, Y. S. Kim: Emeritus

250 mg/L, and residual chlorine (OCl^-) is controlled at 0.1-4 mg/L [14]. The World Health Organization (WHO) also recommends in its drinking water guidelines that chloride (Cl^-) be kept below 250 mg/L and residual chlorine (OCl^-) be maintained in the range of 0.2-5 mg/L [15].

Sodium hypochlorite (NaOCl), which is dosed for drinking water disinfection, dissociates in water into hypochlorous acid (HOCl) and hypochlorite (OCl^-), and the ratio between these two species depends on the solution's pH. Near neutral pH (~7), the more strongly disinfecting HOCl predominates, whereas under alkaline conditions the fraction of OCl^-, which has relatively weaker disinfecting power, increases [16,17]. HOCl can penetrate cell membranes and provides broad-spectrum disinfection against bacteria, viruses, and protozoa. In contrast, OCl^- has lower immediate disinfecting power but remains in the water as a residual to suppress secondary contamination that may occur during distribution [18,19]. Meanwhile, continuous contact of chloride and residual chlorine with the tank interior, together with processes such as evaporation and condensation, can lead to local enrichment of chloride (Cl^-) and residual chlorine (OCl^-), which may act as a factor that increases the likelihood of corrosion [20,21]. From the viewpoint of metallic materials, oxidizing agents such as NaOCl can cause an increase in the open circuit potential (OCP) of metal surfaces [21,22]. As the concentration of oxidizing agents and the exposure time increase, they can affect passive film breakdown and lead localized corrosion [21,23,24]. These factors can induce corrosion at specific areas of stainless steel water tanks. However, systematic studies on this issue are still insufficient.

Therefore, in this study, the effects of ion concentration and temperature on the corrosion behavior of STS 304 base metal and weld metal used for drinking water storage tanks were evaluated electrochemically in simulated drinking water solutions adjusted with NaCl and NaOCl. In addition, the open circuit potential after NaOCl addition was monitored over extended periods and compared with the electrochemical measurements to analyze the causes of corrosion phenomena of type 304 stainless steel occurring in drinking water environments.

2. Experimental Methods

2.1 Materials

The material used in this study was STS 304 stainless steel for drinking water storage tanks, supplied as 1.5 mm-thick plates with the alloy composition listed in Table 1. The base metal and weld metal specimens were provided by Moonchang Co., Ltd. Korea, and were used in the as-received condition without any additional heat treatment. The welded specimens were fabricated by the Gas Tungsten Arc Welding (GTAW) process, using T-308 filler metal with the composition given in Table 2. The detailed welding conditions are summarized in Table 3.

To evaluate the mechanical properties of the base metal, heat-affected zone (HAZ), and weld metal, nanoindentation tests were conducted using a NanoFlip Nanoindenter (Nano-Flip, KLA, USA), and the measured hardness results are presented in Table. 4.

Table 1. Chemical composition of the experimental alloy (wt%)

Alloys	Cr	Ni	C	Si	Mn	Mo	P	S	N	Fe
STS 304	18.25	8.07	0.04	0.45	1.09	0.11	0.03	0.004	0.04	Bal.

Table 2. Chemical composition of filler metal (wt%)

Alloys	Cr	Ni	C	Si	Mn	Mo	Fe
T-308	19.84	9.71	0.04	0.41	1.9	0.17	Bal.

Table 3. Welding condition for the experimental alloy

Process	Voltage (V)	Current (A)	Welding Speed (mm/min)	Heat Input (KJ/mm)	Welding electrode	Shield Gas	Diameter (mm)
GTAW	13-15	150	200	0.4-0.5	W-2.0%Th	Ar(15L/min)	2.4

Table 4. Hardness values of the base metal, HAZ, and weld metal obtained by nanoindentation

Region	Base	HAZ	Weldment
Vickers hardness, HV	336.3	339.9	346.2

2.2 Cyclic polarization test

For electrical connection of the specimens, an insulated copper wire was spot welded to one side and the specimens were then mounted in epoxy resin. After sequential grinding with SiC papers from #80 to #2000, the specimens were insulated with a high-temperature epoxy so that only an area of 1 cm^2 was exposed. To simulate the drinking water environment, test solutions were prepared using NaCl and NaOCl to obtain 50 ppm, 200 ppm, and 400 ppm [Cl^-] and 2 ppm, 4 ppm, and 8 ppm [OCl^-], and the experiments were conducted at 20 ºC, 35 ºC, and 50 ºC. Degassing was not performed because the concentration of residual chlorine (OCl^-) could change during the degassing process. A saturated calomel electrode (SCE) was used as the reference electrode, and a high-density graphite rod was used as the counter electrode. Polarization measurements were carried out using a potentiostat (Interface 1000, Gamry, USA). Polarization was scanned in the anodic direction from the corrosion potential (E_{corr}) at a rate of 1 mV/s, and the scan was reversed when either +900 mV(SCE) or +1 mA/cm^2 was reached. The reverse scan was performed at the same scan rate. The pitting potential (E_p) and protection potential (E_{pro}) were determined as parameters for evaluating corrosion resistance. The protection potential (E_{pro}) is defined as the potential at which the current decreases and rejoins the forward anodic curve during the reverse scan in cyclic polarization, representing the potential at which pits repassivate [25].

2.3 Open Circuit Potential measurement

For electrical connection of the specimens, an insulated copper wire was spot welded to one side, and the specimens were then mounted in epoxy resin. After sequential grinding with SiC papers from #80 to #2000, the specimens were insulated with a high-temperature epoxy so that only an area of 1 cm^2 was exposed. Open-circuit potential (OCP) measurements were performed using a potentiostat (Interface 1000, Gamry, USA). A saturated calomel electrode (SCE) was used as the reference electrode, and a high-density graphite rod was used as the counter electrode. The test solution was prepared with NaCl to obtain a chloride concentration of 200 ppm [Cl^-], corresponding to the maximum level in drinking water, at 20 ºC. OCP was measured from the moment the specimens were immersed in the solution, and after 24 h, NaOCl was added to adjust the residual chlorine to 2 ppm, 4 ppm, or 8 ppm [OCl^-] for each condition, after which the change in OCP was monitored continuously for a total of 144 h.

2.4 Potentiostatic EIS test

For electrical connection of the specimens, an insulated copper wire was spot welded to one side, and the specimens were then mounted in epoxy resin. After sequential grinding with SiC papers from #80 to #2000, the specimens were insulated with a high-temperature epoxy so that only an area of 1 cm^2 was exposed. Electrochemical impedance spectroscopy (EIS) measurements were carried out using a potentiostat (Interface 1000, Gamry, USA), with a saturated calomel electrode as the reference electrode and a high-density graphite rod as the counter electrode. All EIS measurements were conducted at 20 ºC. The measurements were performed at the open-circuit potential over a frequency range from 10 kHz to 0.01 Hz. The specimens were immersed in 200 ppm [Cl^-] solutions containing 2 ppm, 4 ppm, or 8 ppm [OCl^-], and EIS measurements were conducted after 0 h, 24 h, 48 h, 72 h, and 168 h to evaluate how the impedance varied with exposure time at different [OCl^-] concentrations**.** Impedance data (Bode and Nyquist plots) were fitted using a Randles equivalent circuit to extract the solution resistance (R_s), double-layer capacitance (C_{dl}), and polarization resistance (R_p) [26].

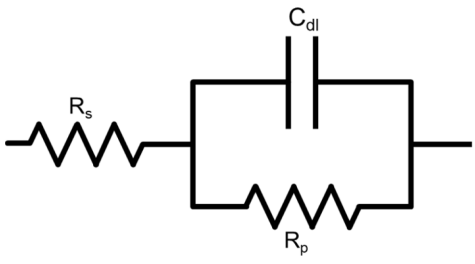

Fig. 1. Randles model [26]

3. Results

Fig. 2 shows the effects of [OCl^-] concentration and temperature (20 ºC, 35 ºC, and 50 ºC) on the cyclic polarization behavior of STS 304 base metal and weld metal. The test solution was 50 ppm [Cl^-] + x ppm [OCl^-] (x = 2, 4, and 8). Fig. 2a and Fig. 2b show the effects of temperature on the cyclic polarization curves of the base metal and weld metal, respectively, in 50 ppm [Cl^-] + 2 ppm [OCl^-]. For the base metal, the corrosion potential tended to decrease as the solution temperature increased, whereas for the weld metal, the Ecorr values at 20 ºC and 50 ºC were similar and lower at 35 °C, showing no monotonic decrease with increasing temperature. For the pitting potential, both materials showed a decreasing trend with increasing temperature. This behavior is attributed to the promotion of passive film breakdown at higher temperatures, which results in a decrease in pitting potential. In contrast, the protection potential showed similar values or scattered behavior depending on the

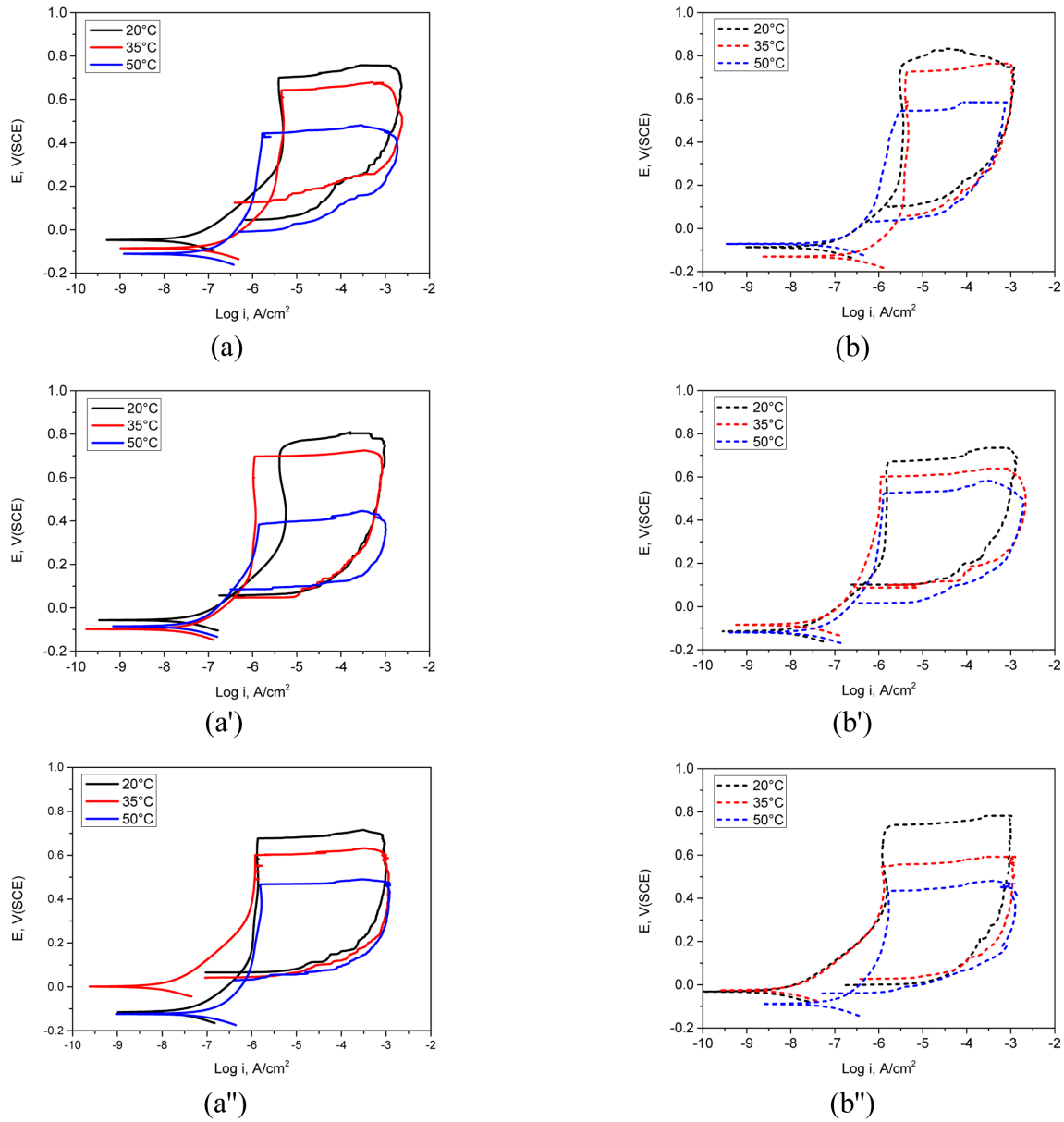

Fig. 2. Effect of OCl^- ion concentration on the cyclic polarization curves of 304 stainless steel (a, a', a") Base metal, (b, b', b") Welded metal in 50 ppm [Cl^-] + x ppm [OCl^-] at each temperature: (a, b) 2 ppm [OCl^-], (a', b') 4 ppm [OCl^-], (a", b") 8 ppm [OCl^-]

condition, and thus the effect of temperature was not consistent.

Fig. 2a' and Fig. 2b' show the effects of temperature on the cyclic polarization curves of the base metal and weld metal, respectively, in 50 ppm [Cl^-] + 4 ppm [OCl^-]. For both the base metal and the weld metal, the corrosion potentials were generally similar irrespective of temperature. For the pitting potential, both materials exhibited a decrease with increasing temperature. The protection potential of the base metal was almost independent of temperature, whereas that of the weld metal was similar at 20 ºC and 35 ºC but decreased at 50 ºC, making the effect of temperature unclear.

Fig. 2a" and Fig. 2b" show the effects of temperature on the cyclic polarization curves of the base metal and weld metal, respectively, in 50 ppm [Cl^-] + 8 ppm [OCl^-]. For the base metal, the corrosion potential was similar at 20 ºC and 50 ºC and higher at 35 ºC. For the weld metal, the corrosion potentials at 20 ºC and 35 ºC were similar, while a lower value was observed at 50 ºC. For both materials, the pitting potential tended to decrease with increasing temperature, and the protection potentials were

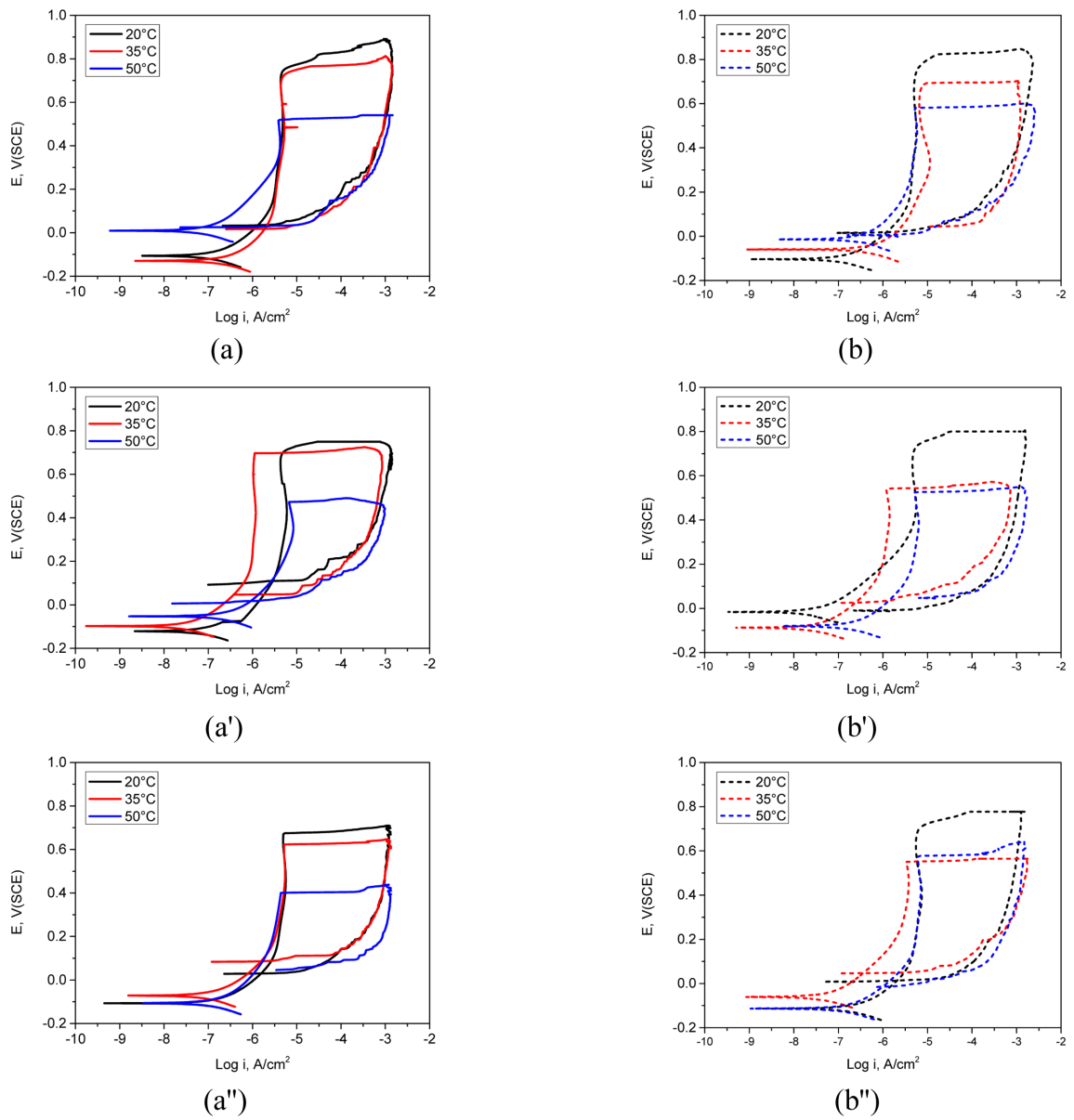

Fig. 3. Effect of OCl^- ion concentration on the cyclic polarization curves of 304 stainless steel (a, a', a") Base metal, (b, b', b") Welded metal in 200 ppm [Cl^-] + x ppm [OCl^-] at each temperature: (a, b) 2 ppm [OCl^-], (a', b') 4 ppm [OCl^-], (a", b") 8 ppm [OCl^-]

similar for both materials.

Fig. 3 shows the effects of [OCl^-] concentration (2 ppm, 4 ppm, and 8 ppm) and temperature (20 ºC, 35 ºC, and 50 ºC) on the cyclic polarization behavior of STS 304 in 200 ppm [Cl^-] + x ppm [OCl^-] solutions.

Fig. 3a and Fig. 3b show the cyclic polarization curves of the base metal and weld metal, respectively, in 200 ppm [Cl^-] + 2 ppm [OCl^-]. The corrosion potential was similar or slightly increased depending on the condition, but no clear trend was observed. For both materials, the pitting potential decreased with increasing temperature, whereas the protection potential was similar irrespective of temperature.

In the case of Fig. 3a' and Fig. 3b', obtained in 200 ppm [Cl^-] + 4 ppm [OCl^-], the temperature dependence of the corrosion potential was not clear for either the base metal or the weld metal, while the pitting potential of both materials decreased with increasing temperature. For the protection potential, a slight decrease with increasing temperature was observed for the base metal, whereas the three values for the weld metal were similar, indicating that the effect of temperature was not consistent.

Fig. 3a" and Fig. 3b", obtained in 200 ppm [Cl^-] + 8 ppm [OCl^-], showed trends similar to those at 2 ppm and 4 ppm [OCl^-]. For both the base metal and weld metal, the corrosion potentials were similar or slightly increased, the pitting potentials decreased, and the protection potentials showed only small variations or similar values. Overall trend is similar to Fig. 2, with the pitting potential decreasing with increasing temperature, while the protection potential showed a small change, making its temperature trend unclear.

Fig. 4 shows the effects of [OCl^-] concentration (2 ppm, 4 ppm, and 8 ppm) and temperature (20 ºC, 35 ºC, and 50 ºC) on the cyclic polarization curves of STS 304 at an increased [Cl^-] concentration of 400 ppm. The measurement procedures and evaluation methods are the same as those used for Fig. 2 and Fig. 3.

In Fig. 4a and Fig. 4b, obtained in 400 ppm [Cl^-] + 2 ppm [OCl^-], the corrosion potentials of both materials were similar, while the pitting potentials decreased with increasing temperature. The protection potential decreased for the base metal but increased for the weld metal, and thus no consistent temperature dependence was observed.

In Fig. 4a' and Fig. 4b', obtained in 400 ppm [Cl^-] + 4 ppm [OCl^-], the corrosion potentials of both the base metal and the weld metal remained similar with increasing temperature, whereas the pitting potentials decreased. For the base metal, the protection potential increased at 35 ºC, so no clear temperature trend was observed. For the weld metal, the three protection potential values were similar.

In Fig. 4a" and Fig. 4b", obtained in 400 ppm [Cl^-] + 8 ppm [OCl^-], the corrosion potentials again showed similar trends, the pitting potentials decreased, and the protection potentials appeared at similar values.

In summary, the cyclic polarization results indicate that even when the [Cl^-] concentration was increased from 50 ppm to 400 ppm, the corrosion potential did not exhibit a consistent change with temperature. In contrast, the pitting potential tended to decrease with increasing temperature under all conditions. The protection potential showed similar values or only small differences among the three temperatures, so a distinct temperature dependence could not be identified.

Fig. 5 summarizes the effects of increasing Cl^- concentration on the pitting potential and protection potential of STS 304 base metal and weld metal, based on values extracted from the cyclic polarization curves in Fig. 2, Fig. 3, and Fig. 4.

Fig. 5a shows the pitting potential and protection potential of STS 304 base metal (B) and weld metal (W) at 20 ºC in 2 ppm [OCl^-] + x ppm [Cl^-] (x = 50, 200, 400). The pitting potential of the base metal was +0.70 V(SCE) at 50 ppm [Cl^-], +0.72 V(SCE) at 200 ppm [Cl^-], and +0.73 V(SCE) at 400 ppm [Cl^-]. These three pitting potential values were similar, showing no significant difference. For the weld metal, the pitting potential was +0.69 V(SCE) at 50 ppm [Cl^-], +0.73 V(SCE) at 200 ppm [Cl^-], and +0.65 V(SCE) at 400 ppm [Cl^-], showing a slight decrease at 400 ppm [Cl^-]. Meanwhile, the protection potential of the base metal was +0.08 V(SCE) at 50 ppm [Cl^-], +0.08 V(SCE) at 200 ppm [Cl^-], and +0.13 V(SCE) at 400 ppm [Cl^-], and the protection potential of the weld metal was +0.08 V(SCE) at 50 ppm [Cl^-], +0.03 V(SCE) at 200 ppm [Cl^-], and +0.14 V(SCE) at 400 ppm [Cl^-]. For the protection potential, both the base metal and weld metal showed higher values at 400 ppm [Cl^-].

Fig. 5a' shows the pitting potential and protection

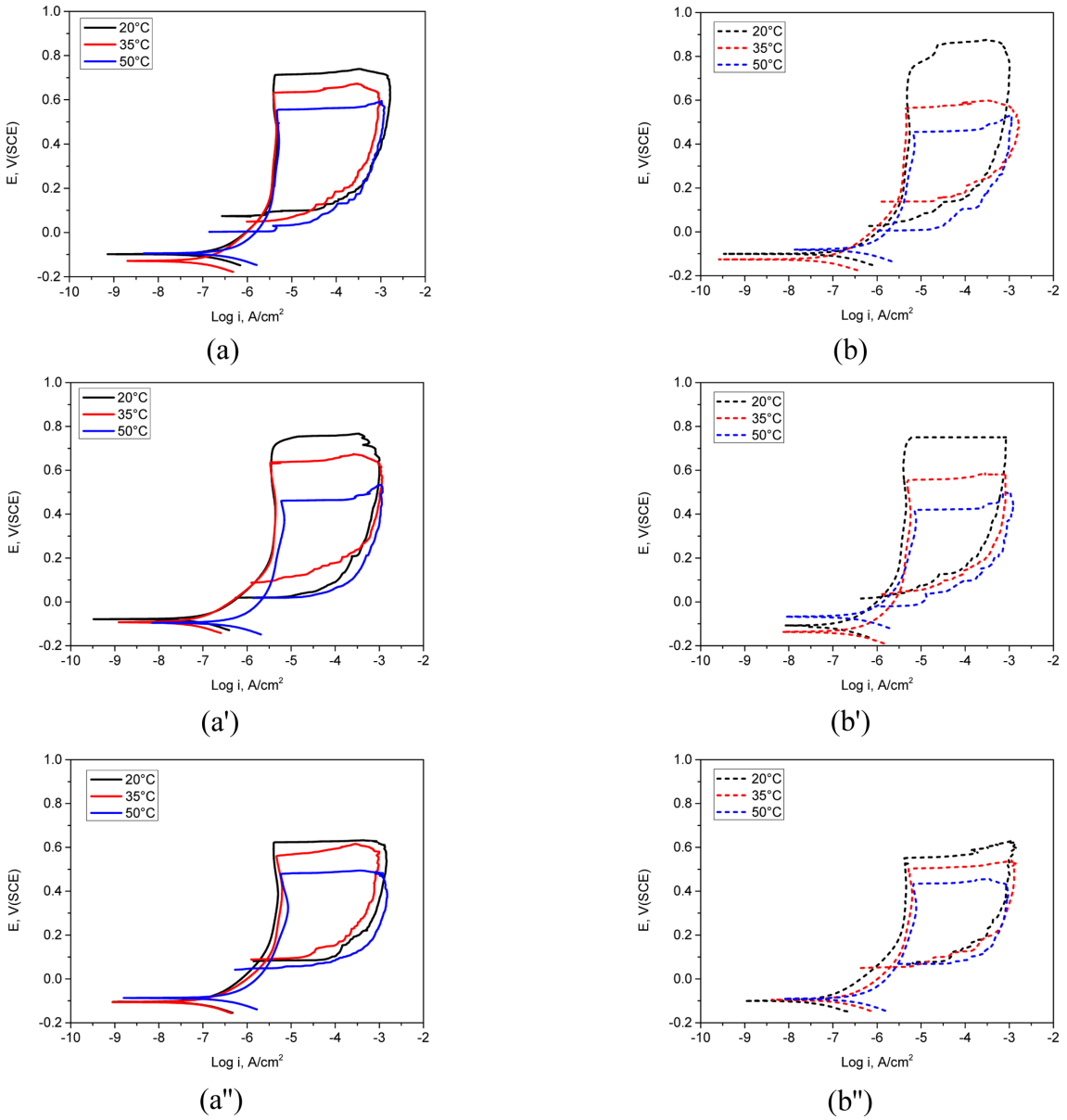

Fig. 4. Effect of OCl^- ion concentration on the cyclic polarization curves of 304 stainless steel (a, a', a") Base metal, (b, b', b") Welded metal in 400 ppm [Cl^-] + x ppm [OCl^-] at each temperature: (a, b) 2 ppm [OCl^-], (a', b') 4 ppm [OCl^-], (a", b") 8 ppm [OCl^-]

potential of STS 304 base metal and weld metal at 20 ºC in 4 ppm [OCl^-] + x ppm [Cl^-] (x = 50, 200, 400). For both the base metal and the weld metal, the pitting potential increased slightly with increasing Cl^- concentration. For the base metal, the protection potential showed only small changes or a slight increase over the entire range, indicating that the effect of Cl^- concentration was not significant. For the weld metal, the protection potential decreased at 200 ppm [Cl^-] and then slightly increased, so the influence of Cl^- concentration was not clear.

Fig. 5a" shows the pitting potential and protection potential of STS 304 base metal and weld metal at 20 ºC in 8 ppm [OCl^-] + x ppm [Cl^-] (x = 50, 200, 400). For both the base metal and the weld metal, the pitting potential tended to decrease slightly at 400 ppm [Cl^-]. In contrast, the protection potentials showed only small variations and similar values, indicating that the effect of Cl^- concentration was not pronounced.

Fig. 5b shows the pitting potential and protection potential of STS 304 base metal and weld metal at 35 ºC

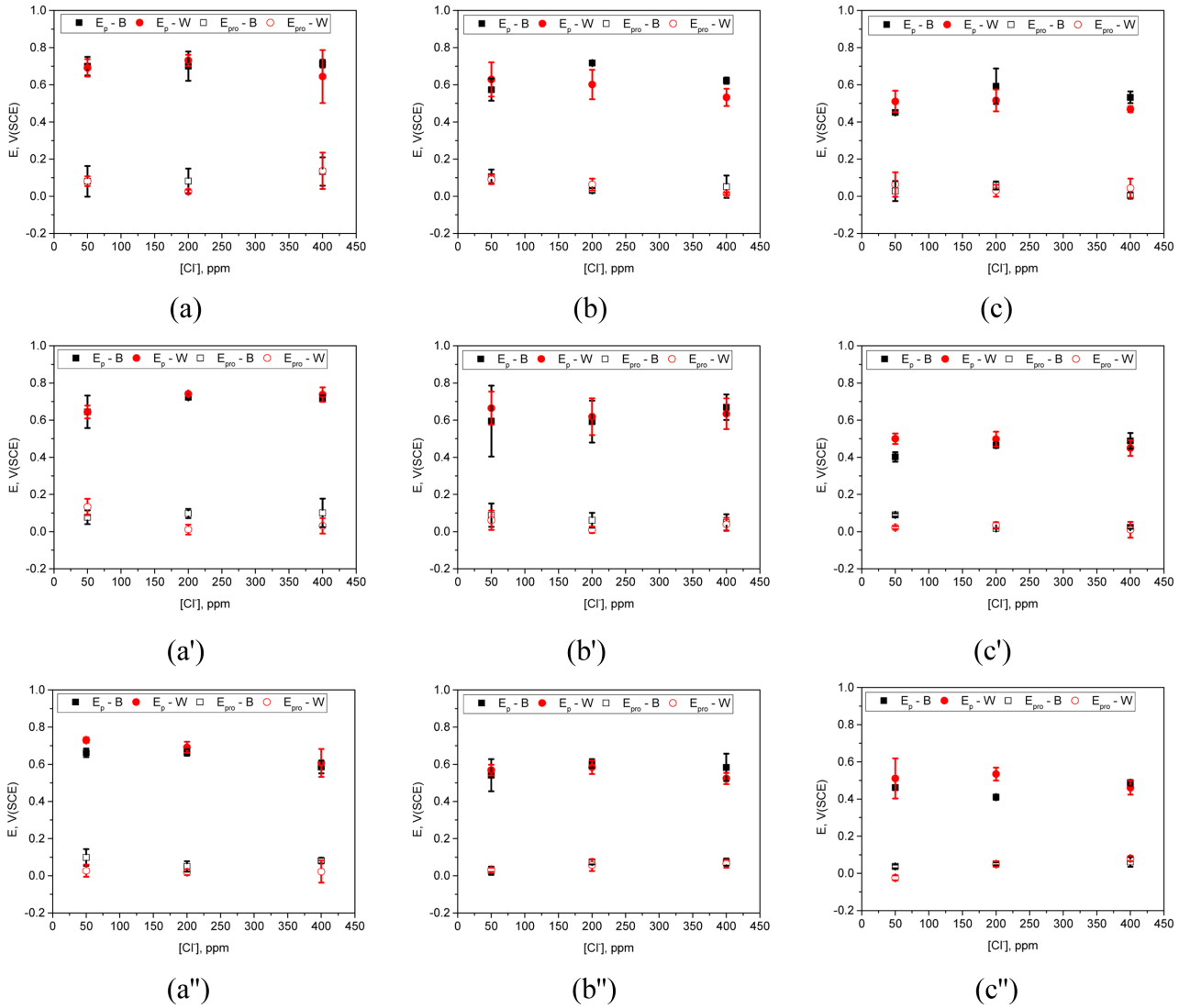

Fig. 5. Effect of Cl^- ion concentration on the pitting potential (E_p) and protection potential (E_{pro}) of 304 stainless steel (B: Base metal, W: Welded metal) in x ppm [Cl^-] + y ppm [OCl^-] at (a, a', a'') 20 °C, (b, b', b'') 35 °C, and (c, c', c'') 50 °C, (a, b, c) 2 ppm [OCl^-], (a', b', c') 4 ppm [OCl^-], (a'', b'', c'') 8 ppm [OCl^-]

in 2 ppm [OCl^-] + x ppm [Cl^-] (x = 50, 200, 400). For the base metal, the pitting potential increased and then decreased at 400 ppm [Cl^-], whereas for the weld metal it decreased with increasing Cl^- concentration. For the protection potential, both the base metal and weld metal showed only small changes, indicating that variations in Cl^- concentration had little effect.

Fig. 5b' shows the pitting potential and protection potential of STS 304 base metal and weld metal at 35 °C in 4 ppm [OCl^-] + x ppm [Cl^-] (x = 50, 200, 400). For both the base metal and weld metal, the pitting potentials were generally similar across the concentrations, with a slight increase at 400 ppm [Cl^-]. For the protection potential, both materials showed similar values, indicating that changes in Cl^- concentration had little effect.

Fig. 5b" shows the pitting potential and protection potential of STS 304 base metal and weld metal at 35 °C in 8 ppm [OCl^-] + x ppm [Cl^-] (x = 50, 200, 400). As the Cl^- concentration increased, the pitting potential of the base metal remained generally similar, and that of the weld metal showed no large difference but decreased slightly at 400 ppm [Cl^-]. For the protection potential, both the base metal and weld metal showed a slight increase with increasing Cl^- concentration, but the values were almost similar, indicating that the influence of Cl^- concentration was minimal.

Fig. 5c shows the pitting potential and protection potential of STS 304 base metal and weld metal at 50 ºC in 2 ppm [OCl^-] + x ppm [Cl^-] (x = 50, 200, 400). For the pitting potential, the base metal showed an increase with increasing Cl^- concentration, whereas the weld metal exhibited similar values without significant changes. For the protection potential, both the base metal and weld metal had similar values, indicating that the effect of increasing Cl^- concentration was not significant.

Fig. 5c' shows the pitting potential and protection potential of STS 304 base metal and weld metal at 50 ºC in 4 ppm [OCl^-] + x ppm [Cl^-] (x = 50, 200, 400). The pitting potential of the base metal increased with increasing Cl^- concentration, whereas that of the weld metal was generally similar across the concentrations. For the protection potential, both the base metal and weld metal exhibited generally similar values, indicating that increasing Cl^- concentration had little influence.

Fig. 5c" shows the pitting potential and protection potential of STS 304 base metal and weld metal at 50 ºC in 8 ppm [OCl^-] + x ppm [Cl^-] (x = 50, 200, 400). For the base metal, the pitting potential showed a slight decrease and then an increase with changing Cl^- concentration. For the weld metal, the three pitting potential values were similar. For the protection potential, both the base metal and weld metal showed a slight increase with increasing Cl^- concentration, but the values were similar, indicating that the effect of concentration was not significant.

In summary, as the Cl^- concentration increased, the pitting potential showed a slight increase or decrease repeatedly under some conditions, but the overall change was minimal and the values were similar, so the effect of the Cl^- concentration could not be clearly identified. The protection potential was also generally similar or showed only small fluctuations, indicating that the effect of Cl^- concentration was limited. Other studies have reported that increasing Cl^- concentration decreases the pitting potential [30,31], and that both increasing temperature and Cl^- concentration decrease the protection potential [32,33]. However, opposite cases have also been reported, in which the effects were unclear due to factors such as reverse scan rate and temperature [34,35]. Considering that the solution compositions used in this study correspond to relatively mild conditions, the influence of increasing Cl^- concentration on the pitting and protection potentials is judged to be limited in such environments.

Fig. 6 summarizes the effects of increasing [OCl^-] on the pitting potential and protection potential of STS 304 base metal and weld metal, based on values extracted from the cyclic polarization curves in Fig. 2, Fig. 3, and Fig. 4.

Fig. 6a shows the pitting potential and protection potential of STS 304 at 20 ºC in 50 ppm [Cl^-] + x ppm [OCl^-] (x = 2, 4, 8). For both the base metal and the weld metal, the pitting potentials were generally similar without significant decreases, and the protection potentials showed only small variations, indicating that the influence of [OCl^-] concentration was limited.

Fig. 6a' shows the pitting potential and protection potential of STS 304 at 20 ºC in 200 ppm [Cl^-] + x ppm [OCl^-] (x = 2, 4, 8). For both the base metal and the weld metal, the pitting and protection potentials were similar without substantial decreases as [OCl^-] increased, suggesting that the effect of concentration was not significant.

Fig. 6a" shows the pitting potential and protection potential of STS 304 at 20 ºC in 400 ppm [Cl^-] + x ppm [OCl^-] (x = 2, 4, 8). For both the base metal and the weld metal, the pitting potentials were similar at 2 ppm and 4 ppm [OCl^-] but decreased at 8 ppm, showing a decreasing tendency with increasing [OCl^-]. For the protection potential, both materials showed slight decreases or similar values with increasing [OCl^-], indicating only a weak concentration effect.

Fig. 6b shows the pitting potential and protection potential of STS 304 at 35 ºC in 50 ppm [Cl^-] + x ppm [OCl^-] (x = 2, 4, 8). Both the pitting and protection potentials showed only small differences with changing [OCl^-], and similar trends were observed for the base metal and weld metal.

Fig. 6b' shows the pitting potential and protection potential of STS 304 at 35 ºC in 200 ppm [Cl^-] + x ppm [OCl^-] (x = 2, 4, 8). For the base metal, the pitting potential tended to decrease slightly with increasing [OCl^-], whereas the weld metal showed generally similar values. For the protection potential, both the base metal and weld metal exhibited similar values, indicating that [OCl^-] concentration had little effect.

Fig. 6b" shows the pitting potential and protection

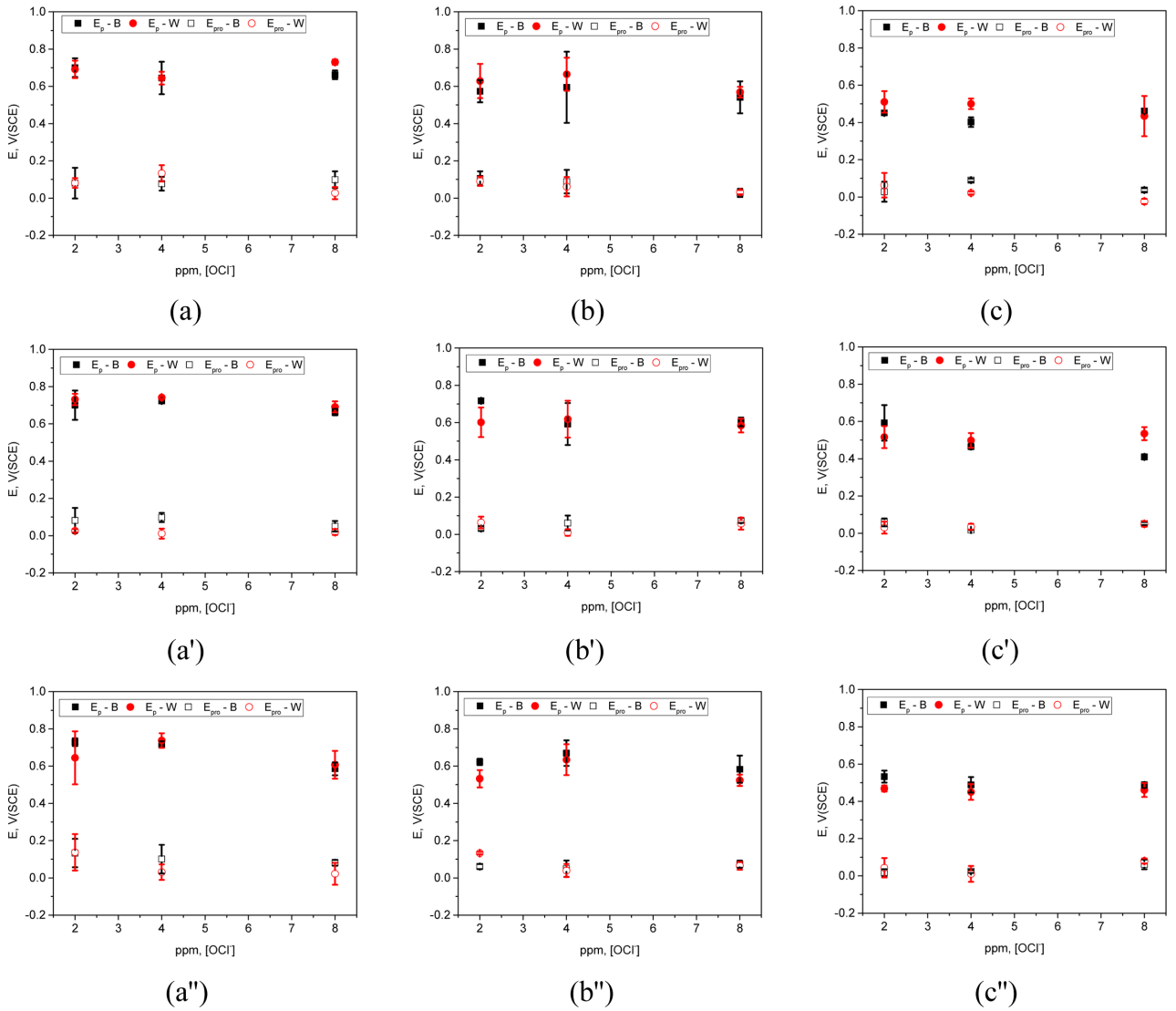

Fig. 6. Effect of OCl^- ion concentration on the pitting potential (E_p) and protection potential (E_{pro}) of 304 stainless steel (B: Base metal, W: Welded metal) in x ppm [Cl^-] + y ppm [OCl^-] at (a, a', a") 20 °C, (b, b', b") 35 °C, and (c, c', c") 50 °C, (a, b, c) 50 ppm [Cl^-], (a', b', c') 200 ppm [Cl^-], (a", b", c") 400 ppm [Cl^-]

potential of STS 304 at 35 °C in 400 ppm [Cl^-] + x ppm [OCl^-] (x = 2, 4, 8). For both the base metal and weld metal, the pitting potentials increased slightly at 4 ppm and then decreased at 8 ppm [OCl^-], so no consistent trend with [OCl^-] concentration was observed. The protection potentials were generally similar for both materials, indicating that the effect of [OCl^-] concentration was small.

Fig. 6c shows the pitting potential and protection potential of STS 304 at 50 °C in 50 ppm [Cl^-] + x ppm [OCl^-] (x = 2, 4, 8). Overall, the weld metal exhibited slightly higher pitting potentials than the base metal, but the changes with [OCl^-] concentration were similar for both materials, indicating a minor influence of [OCl^-]. For the protection potential, the base metal and weld metal showed similar values, again suggesting that [OCl^-] concentration had little effect.

Fig. 6c' shows the pitting potential and protection potential of STS 304 at 50 °C in 200 ppm [Cl^-] + x ppm [OCl^-] (x = 2, 4, 8). For the base metal, the pitting potential tended to decrease as the [OCl^-] concentration increased. For the weld metal, the pitting potentials were generally similar across the concentrations. For the protection potential, both the base metal and weld metal showed

small variations and similar values, implying a limited influence of [OCl^-].

Fig. 6c" shows the pitting potential and protection potential of STS 304 at 50 ºC in 400 ppm [Cl^-] + x ppm [OCl^-] (x = 2, 4, 8). Both the pitting and protection potentials showed no substantial decrease with changing [OCl^-] and had similar values for the base metal and weld metal.

In summary, over all conditions, increasing [OCl^-] did not cause large changes in the pitting or protection potentials. Although slight decreases were observed under some conditions, the overall effect of [OCl^-] concentration was limited. For the protection potential in particular, the changes were generally small, and no distinct effect attributable solely to [OCl^-] was observed.

Fig. 7 presents the effects of temperature on the pitting potential and protection potential of STS 304 base metal and weld metal, using pitting potential and protection potential values determined from the cyclic polarization curves in Fig. 2, Fig. 3, and Fig. 4.

Fig. 7a shows the pitting potential and protection potential of STS 304 at 20 °C, 35 °C, and 50 °C in 50 ppm [Cl^-] + 2 ppm [OCl^-]. For both the base metal and the weld metal, the pitting potential tended to decrease with increasing temperature. For the protection potential, both materials showed small and similar changes, indicating that the effect of temperature was limited.

Fig. 7a' shows the pitting potential and protection potential of STS 304 at 20 °C, 35 °C, and 50 °C in 50 ppm [Cl^-] + 4 ppm [OCl^-]. For both the base metal and the weld metal, the pitting potential decreased with increasing temperature. The protection potentials were similar across the temperatures, and no significant temperature effect was observed.

Fig. 7a" shows the pitting potential and protection potential of STS 304 at 20 °C, 35 °C, and 50 °C in 50 ppm [Cl^-] + 8 ppm [OCl^-]. As the temperature increased, the pitting potentials of both the base metal and the weld metal decreased. The protection potentials of both materials exhibited similar values, indicating that temperature had little effect.

Fig. 7b shows the pitting potential and protection potential of STS 304 at 20 °C, 35 °C, and 50 °C in 200 ppm [Cl^-] + 2 ppm [OCl^-]. For both the base metal and the weld metal, the pitting potential decreased as the temperature increased. For the protection potential, both materials showed similar values with little change, suggesting a small effect of temperature.

Fig. 7b' shows the pitting potential and protection potential of STS 304 at 20 °C, 35 °C, and 50 °C in 200 ppm [Cl^-] + 4 ppm [OCl^-]. For both the base metal and the weld metal, the pitting potential tended to decrease with increasing temperature. The protection potentials of the base metal and weld metal were similar and showed no significant change with temperature.

Fig. 7b" shows the pitting potential and protection potential of STS 304 at 20 °C, 35 °C, and 50 °C in 200 ppm [Cl^-] + 8 ppm [OCl^-]. For both the base metal and weld metal, the pitting potential decreased as the temperature increased. For the protection potential, the values remained almost unchanged with increasing temperature.

Fig. 7c shows the pitting potential and protection potential of STS 304 at 20 °C, 35 °C, and 50 °C in 400 ppm [Cl^-] + 2 ppm [OCl^-]. For both the base metal and the weld metal, the pitting potential showed a decreasing trend with increasing temperature. The protection potentials of both materials also tended to decrease as the temperature increased.

Fig. 7c' shows the pitting potential and protection potential of STS 304 at 20 °C, 35 °C, and 50 °C in 400 ppm [Cl^-] + 4 ppm [OCl^-]. For the pitting potential, both the base metal and the weld metal showed decreasing values with increasing temperature. For the protection potential, a slight decrease was observed with increasing temperature, but the values were generally similar.

Fig. 7c" shows the pitting potential and protection potential of STS 304 at 20 °C, 35 °C, and 50 °C in 400 ppm [Cl^-] + 8 ppm [OCl^-]. As the temperature increased, the pitting potentials of both the base metal and the weld metal decreased. For the protection potential, the base metal and weld metal exhibited similar values, indicating that temperature had little effect.

In summary, overall, the pitting potential decreased with increasing temperature for both the base metal and the weld metal. This is considered to be due to the acceleration of diffusion and dissolution reactions at higher temperatures, which increases the susceptibility to pit initiation. In contrast, the protection potential showed only small changes, indicating that the influence of temperature

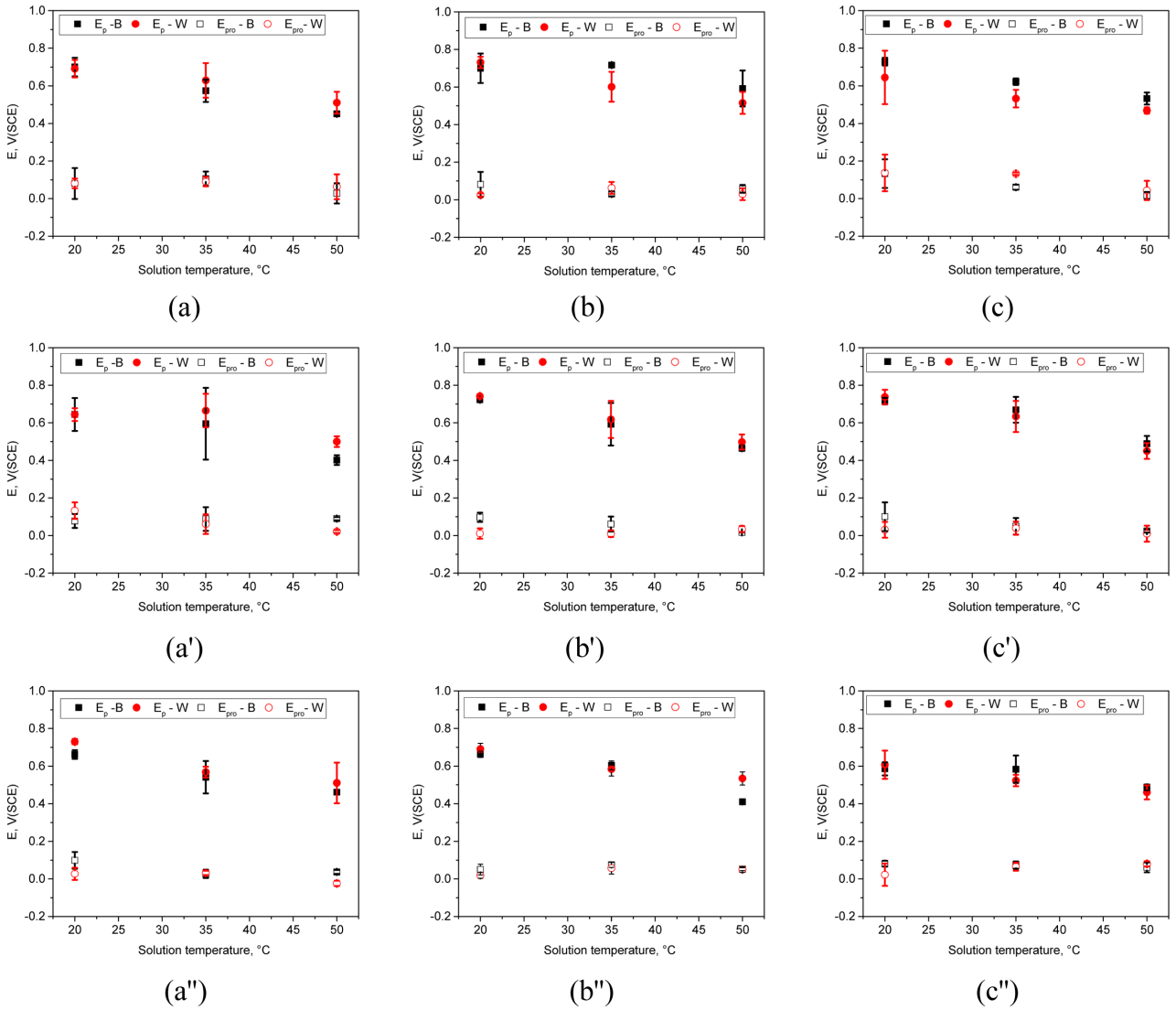

Fig. 7. Effect of temperature (20 °C, 35 °C, and 50 °C) on the pitting potential (E_p) and protection potential (E_{pro}) of 304 stainless steel (B: Base metal, W: Welded metal) in x ppm [Cl^-] + y ppm [OCl^-] at (a, a', a'') 50 ppm [Cl^-], (b, b', b'') 200 ppm [Cl^-], and (c, c', c'') 400 ppm [Cl^-], (a, b, c) 2 ppm [OCl^-], (a', b', c') 4 ppm [OCl^-], (a'', b'', c'') 8 ppm [OCl^-]

was not significant. This is likely because the solution compositions used in this study correspond to relatively low (mild) concentrations.

For direct numerical comparison, the E_p and E_{pro} values extracted from the cyclic polarization curves in Fig. 5, Fig. 6 and Fig. 7 are presented in Table 5 and Table 6.

4. Discussion

As described the above, despite the increase in Cl^- concentration in the solution, no clear trend was observed in either the pitting potential or the protection potential. Changes in OCl^- concentration also had little effect on E_p and E_{pro}. This is considered to be due to the fact that the simulated drinking water solutions used in this study correspond to relatively mild conditions. In contrast, increasing temperature generally lowered the pitting potential, whereas the protection potential was not significantly affected. In other words, under most conditions in this study, the E_p and E_{pro} values of the base metal and weld metal were similar to each other. Meanwhile, in actual service environments, if the open-circuit potential increases, or if Cl^- enrichment and crevice formation occur, corrosion can develop at certain locations

Table 5. Pitting potential (E_p) and protection potential (E_{pro}) obtained from cyclic polarization tests for STS 304B (Base metal) under various [Cl^-], [OCl^-] concentrations and temperature

Specimen	[Cl^-], ppm	[OCl^-], ppm	Temperature, °C	E_p, V(SCE)	E_{pro}, V(SCE)
STS 304B	50	2	20	0.70	0.08
			35	0.57	0.11
			50	0.45	0.03
		4	20	0.64	0.08
			35	0.60	0.09
			50	0.40	0.09
		8	20	0.66	0.10
			35	0.54	0.03
			50	0.46	0.04
STS 304B	200	2	20	0.70	0.08
			35	0.72	0.03
			50	0.59	0.06
		4	20	0.72	0.10
			35	0.59	0.06
			50	0.47	0.02
		8	20	0.66	0.05
			35	0.60	0.07
			50	0.41	0.05
STS 304B	400	2	20	0.73	0.13
			35	0.62	0.06
			50	0.53	0.02
		4	20	0.72	0.10
			35	0.67	0.05
			50	0.49	0.02
		8	20	0.59	0.08
			35	0.58	0.07
			50	0.49	0.06

in drinking water facilities made of 304 stainless steel [20,21,27,28].

To analyze the causes of these phenomena, the open-circuit potential was monitored over an extended period after the addition of [OCl^-] in simulated drinking water solutions. Fig. 8 shows the OCP results measured continuously for 168 h at 20 °C in a 200 ppm [Cl^-] solution, while varying the [OCl^-] concentration to 2, 4, and 8 ppm and stirring at 120 rpm. As shown in Fig. 8a, for the base metal, the OCP remained in the range from –0.1 V(SCE) to 0 V(SCE) during the first 24 h before [OCl^-] addition, but increased markedly with time immediately after [OCl^-] was added. When 2 ppm [OCl^-] was added, the potential increased rapidly and reached approximately +0.32 V(SCE) after 168 h. At 4 ppm and 8 ppm [OCl^-], the OCP reached about +0.37 V(SCE) and +0.48 V(SCE), respectively. The weld metal showed overall similar behavior to the base metal, as presented in Fig. 8b. Before [OCl^-] addition, the OCP ranged between –0.1 V(SCE) and +0 V(SCE), but it increased significantly after [OCl^-] was added. With 2 ppm [OCl^-], the potential reached +0.32 V(SCE) after 168 h, with 4 ppm

Table 6. Pitting potential (E_p) and protection potential (E_{pro}) obtained from cyclic polarization tests for STS 304W (Welded metal) under various [Cl^-], [OCl^-] concentrations and temperature

Specimen	[Cl^-], ppm	[OCl^-], ppm	Temperature, °C	E_p, V(SCE)	E_{pro}, V(SCE)
STS 304W	50	2	20	0.69	0.08
			35	0.63	0.09
			50	0.51	0.06
		4	20	0.64	0.13
			35	0.67	0.06
			50	0.50	0.02
		8	20	0.73	0.03
			35	0.57	0.03
			50	0.51	-0.02
STS 304W	200	2	20	0.73	0.03
			35	0.60	0.06
			50	0.52	0.03
		4	20	0.74	0.01
			35	0.62	0.01
			50	0.50	0.03
		8	20	0.69	0.02
			35	0.58	0.06
			50	0.53	0.05
STS 304W	400	2	20	0.64	0.14
			35	0.53	0.13
			50	0.47	0.04
		4	20	0.74	0.03
			35	0.63	0.04
			50	0.45	0.01
		8	20	0.61	0.02
			35	0.52	0.07
			50	0.46	0.08

[OCl^-], it reached +0.40 V(SCE) after 168 h, and with 8 ppm [OCl^-], it reached +0.43 V(SCE) after 168 h. For both the base metal and the weld metal, the OCP increased in a similar manner with increasing [OCl^-] concentration.

This behavior is attributed to [OCl^-] acting as an oxidizing agent in the solution, thereby increasing the metal potential [21,23,29]. In other words, [OCl^-] rapidly promotes the formation of a passive film on the surface, temporarily suppressing metal dissolution and consequently raising the OCP.

Since the addition of [OCl^-] can increase the open-circuit potential and thereby promote passivation, the change in passive film resistance with exposure time was evaluated by potentiostatic EIS tests, in which the polarization resistance was determined at specific times before and after [OCl^-] addition. Fig. 9 shows the R_p values measured for STS 304 base metal and weld metal at 20 °C in a 200 ppm [Cl^-] solution, before [OCl^-] addition (0 h) and at 24 h, 48 h, 72 h, and 168 h after the addition of 2 ppm, 4 ppm, or 8 ppm [OCl^-]. Fig. 9a shows the change in polarization resistance of the STS 304 base metal as a function of [OCl^-] concentration. At 2 ppm

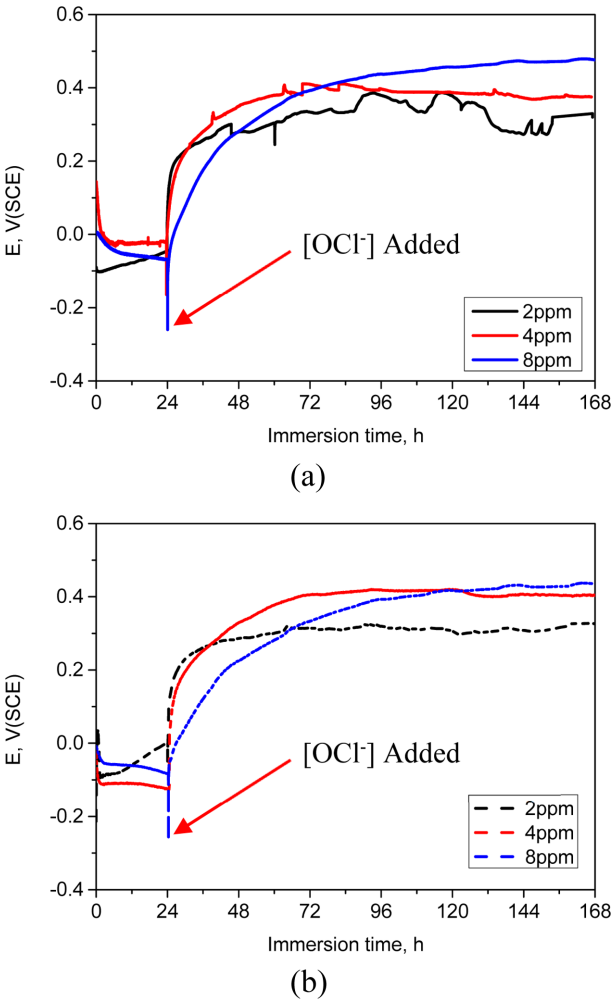

Fig. 8. Effect of [OCl⁻] ion injection on the open circuit potential of 304 stainless steel in 200 ppm [Cl⁻] + x ppm [OCl⁻] at 20 °C: (a) Base metal, (b) Welded metal

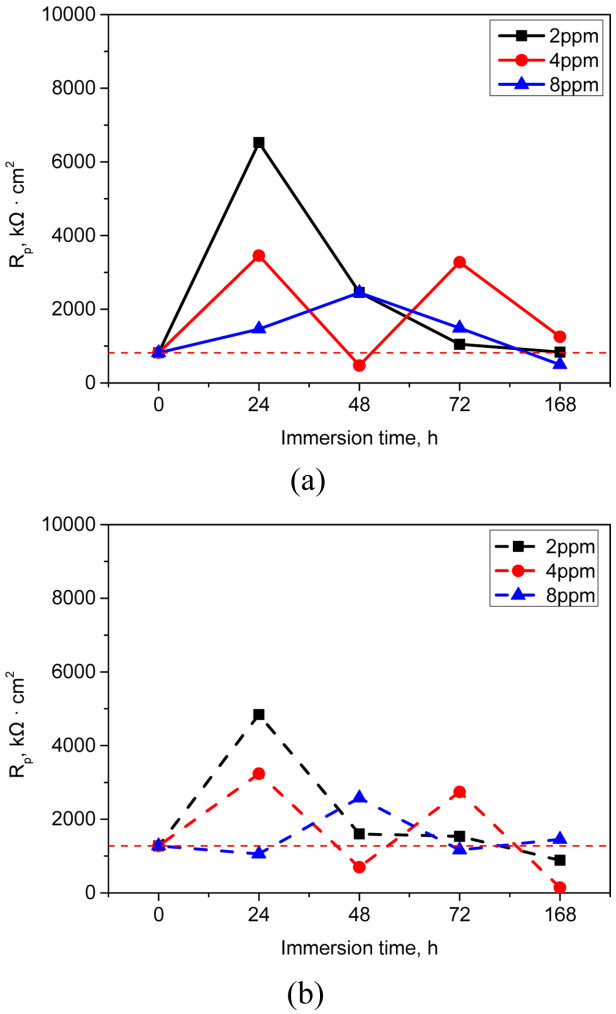

Fig. 9. Effect of the immersion time after [OCl⁻] ion injection on the polarization resistance obtained by EIS test of 304 stainless steel in 200 ppm [Cl⁻] + x ppm [OCl⁻] at 20 °C: (a) Base metal, (b) Welded metal

[OCl^-], R_p increased at 24 h after addition, but then decreased and returned to a level similar to that before addition. At 4 ppm [OCl^-], R_p repeatedly increased and decreased with time, showing no clear trend, and at 168 h it was close to the initial value. At 8 ppm [OCl^-], R_p increased up to 48 h and then decreased, becoming similar to the initial value. Fig. 9b shows the potentiostatic EIS results for the STS 304 weld metal, which exhibited trends similar to those of the base metal in Fig. 9a. After the addition of 2 ppm [OCl^-], R_p increased at 24 h and then decreased. At 4 ppm [OCl^-], R_p repeatedly increased and decreased with time after [OCl^-] addition and eventually became slightly lower than the pre-addition level. At 8 ppm [OCl^-], R_p reached a maximum at 48 h and then decreased, resulting in a value similar to that before addition. Thus, after [OCl^-] addition, R_p showed a temporary increase within 48 h followed by a decrease or fluctuation, and no consistent overall trend was observed.

This behavior is considered to result from the oxidizing effect of [OCl^-] in a relatively mild corrosive environment, which temporarily enhances the passive film on the metal surface and increases R_p, but the effect weakens over time and R_p returns to its pre-addition level. Therefore, in this solution it is difficult to attribute corrosion directly to continuous strengthening or weakening of the passive film by [OCl^-] itself. In other words, the addition of [OCl^-] initially raises the open-circuit potential of 304 stainless steel to a more noble level and enhances the stability of

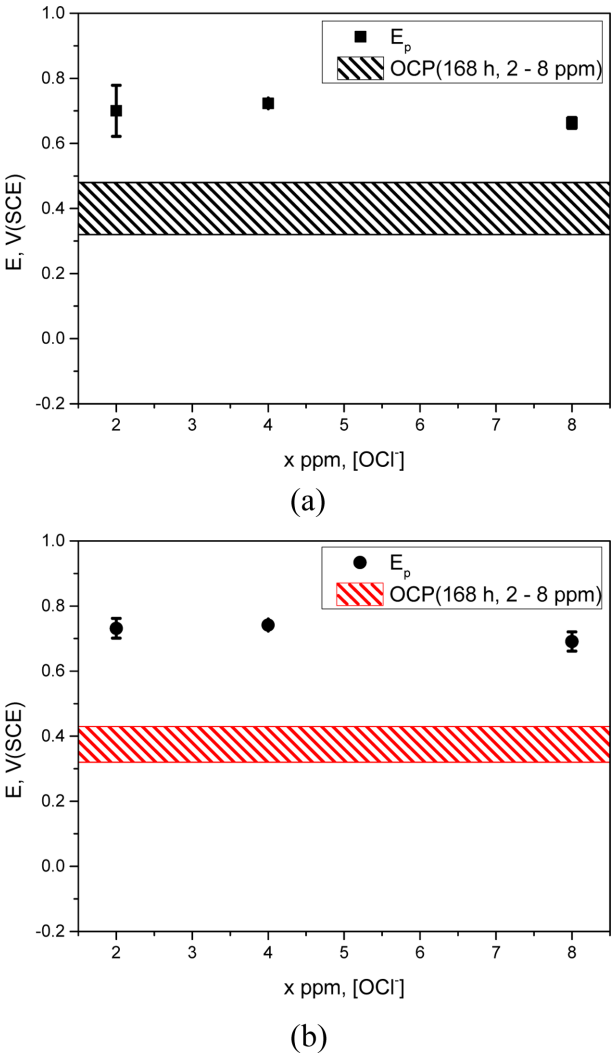

Fig. 10. Corrosion possibility analysis based on the relationship between pitting potential (■, ●) and OCP (band) of stainless steel after 168 h of [OCl⁻] injection in 200 ppm [Cl⁻] + 2 ~ 8 ppm [OCl⁻]: (a) Base metal, (b) Welded metal

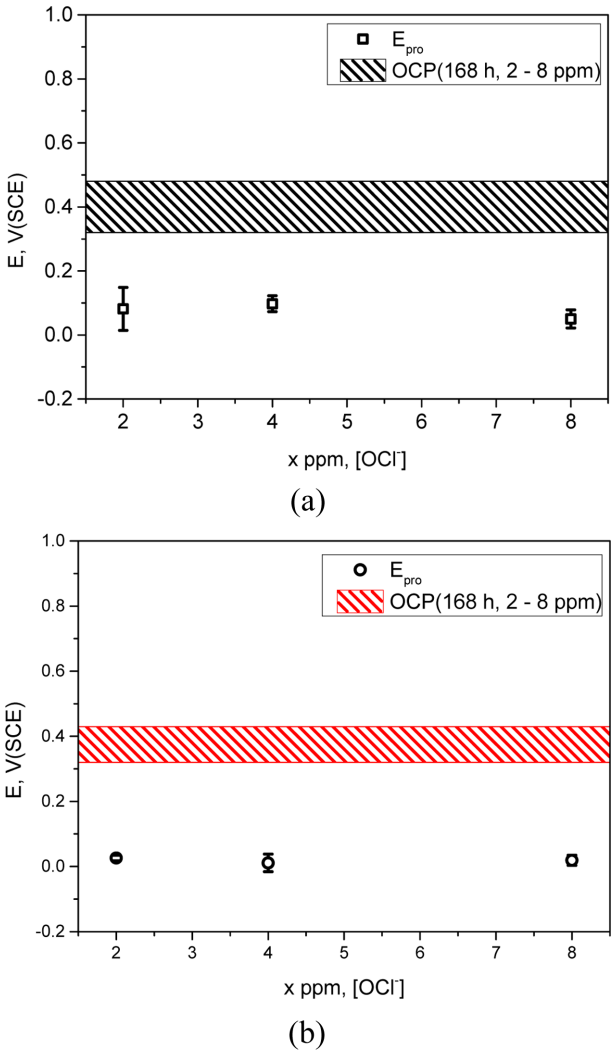

Fig. 11. Corrosion possibility analysis based on the relationship between protection potential (□, ○) and OCP band of stainless steel after 168 h of [OCl⁻] injection in 200 ppm [Cl⁻] + 2 ~ 8 ppm [OCl⁻]: (a) Base metal, (b) Welded metal

the passive film, but this effect diminishes with time and the potential becomes similar to the pre-addition value.

Then, why does corrosion damage occur in drinking water facilities made of 304 stainless steel? To clarify this, attention was focused on the changes in potential caused by [OCl⁻] addition. Fig. 10 shows the pitting potentials of STS 304 base metal and weld metal in 200 ppm [Cl⁻] + 2 ~ 8 ppm [OCl⁻] solutions, together with the bands of increased open-circuit potential at 168 h after adding 2~8 ppm [OCl⁻] to a 200 ppm [Cl⁻] solution. Fig. 10a compares the pitting potential of the STS 304 base metal with the OCP to evaluate the likelihood of pit initiation. For the base metal, the OCP band ranged from +0.32 V(SCE) to +0.48 V(SCE) across the tested conditions. For all conditions, the pitting potentials were higher than the increased open-circuit potentials, regardless of [OCl⁻] concentration. From the standpoint of pitting potential, this indicates that even though the OCP increases, it does not reach E_p, and thus pit initiation is not expected under these conditions. In addition, Fig. 10b compares the pitting potential of the STS 304 weld metal with the OCP to evaluate the likelihood of pit initiation. For the weld metal, the OCP band ranged from +0.32 V(SCE) to +0.43 V(SCE) across the tested conditions. It shows trends similar to those of the base metal. At all [OCl⁻] concentrations, the OCP did not reach the pitting potential. This suggests that, from

the perspective of pitting potential and increased OCP, the likelihood of pit initiation is also low in the weld metal.

Meanwhile, Fig. 11a and Fig. 11b show the protection potentials of STS 304 base metal and weld metal in 200 ppm [Cl^-] + 2 ~ 8 ppm [OCl^-] solutions, together with the bands of increased OCP at 168 h after adding 2 ~ 8 ppm [OCl^-] to a 200 ppm [Cl^-] solution. For the OCP bands at 168 h, the base metal ranged from +0.32 V(SCE) to +0.48 V(SCE), and the weld metal ranged from +0.32 V(SCE) to +0.43 V(SCE). As can be seen in Fig. 11, the bands of increased OCP after [OCl^-] addition were higher than the protection potentials of both the base metal and the weld metal. In other words, the fact that the OCP increased by [OCl^-] addition exceeds the protection potential of stainless steel implies that pitting can occur during long-term service in such environments. Therefore, the corrosion damage observed in 304 stainless steel used in drinking water facilities is considered to result from the strong oxidizing power of [OCl^-] ions used in water treatment, which raises the open-circuit potential above the protection potential.

5. Conclusions

In this study, the corrosion behavior of STS 304 base metal and weld metal used for potable water storage tanks was evaluated under simulated potable-water conditions by varying [Cl^-], [OCl^-], and temperature, and the following conclusions were obtained.

1. From the cyclic polarization tests, variations in [Cl^-] and [OCl^-] had no significant effect on the pitting potential or the protection potential. An increase in solution temperature decreased the pitting potential, but did not appear to exert a clear influence on the protection potential. This behavior is attributed to accelerated diffusion and dissolution reactions at higher temperatures, which increase the susceptibility to pit initiation, while the relatively low ion concentrations used in this study limit the overall impact.

2. The open-circuit potential increased by [OCl^-] ions used as a drinking water disinfectant was found to lie above the protection potential and below the pitting potential of 304 stainless steel, and the polarization resistance increased. Therefore, the corrosion damage observed in 304 stainless steel used in drinking water facilities is considered to be closely related to the strong oxidizing power of [OCl^-] ions during water treatment, which raises the open-circuit potential above the protection potential.

Acknowledgement

This work was supported by the 2023 Technology Development Program funded by the Ministry of SMEs and Startups (Korea) [S3377264].) The authors also gratefully acknowledge the support of MoonChang Co., Ltd.

References

1. M. W. LeChevallier, K. K. Au, Water treatment and pathogen control: process efficiency in achieving safe drinking water, *Geneva: WHO & IWA Publishing* (2004).
2. W. A. M. Hijnen, E. F. Beerendonk and G. J. Medema, Inactivation credit of UV radiation for viruses, bacteria and protozoan (oo)cysts in water: A review, *Water Research*, **40**, 3 (2006). Doi: https://doi.org/10.1016/j.watres.2005.10.030
3. M. Lau, P. T. Monis and B. J. King, The efficacy of current treatment processes to remove, inactivate, or reduce environmental bloom-forming Escherichia coli, *Microbiology Spectrum*, **12**, 24 (2024). Doi: https://doi.org/10.1128/spectrum.00856-24
4. V. G. Alvarez, Field- and pilot-scale approaches to assess finished water storage tanks, *Journal of the American Water Works Association*, **115**, 24 (2023). Doi: https://doi.org/10.1002/awwa.2196
5. E. Demirel, M. M. Aral, An efficient contact tank design for potable water treatment, *İMO Teknik Dergi*, **29**, 8279 (2018). Doi: https://doi.org/10.18400/tekderg.322491
6. R. E. Avery, S. Lamb, C. A. Powell, and A. H. Tuthill, Stainless steel for potable water treatment plants (PWTPs), *Nickel Institute Technical Series*, 10087 (1999).
7. S. L. Percival, J. L. Beech, R. G. J. Edyvean, J. S. Knapp and D. S. Wales, Biofilm development on 304 and 316 stainless steels in a potable water system, *Chartered Institution of Water and Environmental Management*, **11**, 289 (1997). Doi: https://doi.org/10.1111/j.1747-6593.1997.tb00131.x
8. S. L. Percival, J. S. Knapp, R. G. J. Edyvean, D. S. Wales, Biofilms, mains water and stainless steel, *Water Research*, **32**, 2187 (1998). Doi: https://doi.org/10.1016/S0043-1354(97)00415-6

9. T. Hong, M. Nagumo, The effect of chloride concentration on early stages of pitting for type 304 stainless steel revealed by the AC impedance method, *Corrosion Science*, **39**, 285 (1997). Doi: https://doi.org/10.1016/S0010-938X(96)00127-8
10. Z. Yin, Effect of chloride ion concentration on the corrosion behavior of 304 stainless steel used in the electric water heater, *Intternational Journal of Electrochemical Science*, **17**, 220415 (2022). Doi: https://doi.org/10.20964/2022.04.31
11. R. T. Loto, S. Oladipupo, T. Folarin and E. Okusun, Impact of chloride concentrations on the electrochemical performance and corrosion resistance of austenitic and ferritic stainless steels in acidic chloride media, *Discover Applied Sciences*, **7**, 672 (2025). Doi: https://doi.org/10.1007/s42452-025-07234-4
12. E. A. Add El Meguid, N. A. Mahmoud and V. K. Gouda, Pitting corrosion behaviour of AISI 316L steel in chloride containing solutions, *British Corrosion Journal*, **33**, 42 (1998). Doi: https://doi.org/10.1179/000705998798114787
13. S. H. Mameng, R. Pettersson and J. Y. Jonson, Limiting conditions for pitting corrosion of stainless steel EN 1.4404 (316L) in terms of temperature, potential and chloride concentration, *Materials and Corrosion*, **68**, 272 (2017). Doi: https://doi.org/10.1002/maco.201609061
14. K. Jinkeun, H. J. An, Rechlorination for residual chlorine concentration equalization in distribution system, *Journal of Korean Society of Water and Wastewater*, **28**, 91 (2014). Doi: http://dx.doi.org/10.11001/jksww.2014.28.1.91
15. C. Onyutha, J. C. K. Tamale, Modelling chlorine residuals in drinking water: a review, *International Journal of Environmental Science and Technology*, **19**, 11613 (2022). Doi: https://doi.org/10.1007/s13762-022-03924-3
16. G. R. Fedele, A. R. Guastalli, E. J. Doğramacı, L. Steier and J. A. P. De Figueiredo, Influence of pH changes on chlorine-containing endodontic irrigating solutions. *International Endodontic Journal*, **44**, 792 (2011). Doi: https://doi.org/10.1111/j.1365-2591.2011.01911.x
17. S. Fukuzaki, Mechanisms of actions of sodium hypochlorite in cleaning and disinfection processes. *Biocontrol Science*, **11**, 147 (2006). Doi: https://doi.org/10.4265/bio.11.147
18. T. B. Sil, D. Malyshev, M. Aspholm, M. Andersson, Boosting hypochlorite's disinfection power through pH modulation, *BMC Microbiology*, **25**, 101 (2025). Doi: https://doi.org/10.1186/s12866-025-03831-w
19. M. S. Block , B. G. Rowan, Hypochlorous acid: A review. *Journal of Oral and Maxillofacial Surgery*, **78**, 1461 (2020). Doi: https://doi.org/10.1016/j.joms.2020.06.029
20. C. M. B. Martins, J. L. Moreira and J. I. Martins, Corrosion in water supply pipe stainless steel 304 and a supply line of helium in stainless steel 316. *Engineering Failure Analysis*, **39**, 65 (2014). Doi: https://doi.org/10.1016/j.engfailanal.2014.01.017
21. K. Li, L. Sun, W. Cao, S. Chen, Z. Chen, W. Yanli and W. Li, Pitting corrosion of 304 stainless steel in secondary water supply system. *Corrosion Communications*, **7**, 43 (2022). Doi: https://doi.org/10.1016/j.corcom.2021.11.010
22. S. Mameng, R. Pettersson, Localised corrosion of stainless steels depending on chlorine dosage in chlorinated water, *EUROCORR 2011*, Stockholm, Sweden 4-8 (2011). Doi: http://urn.kb.se/resolve?urn=urn:nbn:se:kth:diva-263815
23. G. Tranchida, F. Di Franco, S. Virtanen, M. Santamaria, Effect of NaClO disinfection/cleaning on passive films on AISI 316L. *Corrosion Science*, **165**, 108415 (2020). Doi: https://doi.org/10.1016/j.corsci.2019.108415
24. R. D. Costa, M. L. Barbosa, F. J. Silva, S. R. Sousa, V. F. Sousa and B. O. Ferreira, Study of the chlorine influence on the corrosion of three steels to be used in water treatment municipal facilities, *Materials*, **16**, 2514 (2020). Doi: https://doi.org/10.3390/ma16062514
25. H. K. Hwang, S. J. Kim, Effect of temperature on electrochemical characteristics of stainless steel in green death solution using cyclic potentiodynamic polarization test, *Corrosion Science and Technology*, **20**, 266 (2021). Doi: https://doi.org/10.14773/cst.2021.20.5.266
26. ASTM G3-04, Standard practice for conventions applicable to electrochemical measurements in corrosion testing, *ASTM International : West Conshohocken, PA, USA* (2004).
27. D. A. Moreno, A. M. Garcia, C. Ranninger and B. Molina, Pitting corrosion in austenitic stainless steel water tanks of hotel trains, *Revista De Metalurgia*, **47**, 497 (2011). Doi: https://doi.org/10.3989/revmetalm.1146
28. E. E. Mackey, T. F. Seacord, Guidelines for using stainless steel in the water and desalination industries, *Journal AWWA*, **109**, 158 (2017). Doi:https://doi.org/10.5942/jawwa.2017.109.0044
29. N. Larché, C. Leballeur, L. Manchet, S. L. Manchet and W. He, Localized Corrosion of high-grade stainless steels: grade selection in chlorinated seawater, *Corrosion*, **79**, 997 (2023). Doi: https://doi.org/10.5006/4348
30. M. A. M. Ibrabim, S. S. E. Rehim, M. M. Hamza, Corrosion behavior of some austenitic stainless steels in

chloride environments, *Materials Chemistry and Physics*, **115**, 80 (2009). Doi: https://doi.org/10.1016/j.matchemphys.2008.11.016

31. H. P. Leckie, H. H. Uhlig, Environmental factors affecting the critical potential for pitting in 18-8 stainless steel, *Journal of The Electrochemical Society*, **113**, 1262 (1966). Doi: https://doi.org/10.1149/1.2423801
32. K. V. S. Ramana, T. Anita, S. Mandal, S. Kaliappan, H. Shaikh, P. V. Sivaprasad, R. K. Dayal and H. S. Khatak, Effect of different environmental parameters on pitting behavior of AISI type 316L stainless steel: Experimental studies and neural network modeling, *Materials and Design*, **30**, 3770 (2009). Doi: https://doi.org/10.1016/j.matdes.2009.01.039
33. S. Tsujikawa, S. Okayama, Repassivation method to determine critical conditions in terms of electrode potential, temperature and NaCl concentration to predict crevice corrosion resistance of stainless steels, *Corrosion Science*, **31**, 441 (1990). Doi: https://doi.org/10.1016/0010-938X(90)90143-S
34. N. Sridhar, G. A. Cragnolino, Applicability of repassivation potential for long-term prediction of localized corrosion of alloy 825 and type 316L stainless steel, *Corrosion*, **49**, 885 (1993). Doi: https://doi.org/10.5006/1.3316014
35. S. Esmailzadeh, M. Aliofkhazraei, and H. Sarlak, Interpretation of cyclic potentiodynamic polarization test results for study of corrosion behavior of metals: A review, *Protection of Metals and Physical Chemistry of Surfaces*, **54**, 976 (2018). Doi: https://doi.org/10.1134/S207020511805026X